ARCHIVE OF MECHANICAL ENGINEERING

DOI: 10.24425/ame.2023.148700 2023, Vol. 70, No. 4, pp. 567–587

Allaeddine Yahia DAMANI [1], Zoubir Abdeslem BENSELAMA [1], Ramdane HEDJAR [2]

Formation control of nonholonomic wheeled mobile robots using adaptive distributed fractional order fast terminal sliding mode control

Received 15 October 2023, **Revised** 12 December 2023, **Accepted** 20 December 2023, **Published online** 28 December 2023

Keywords: mobile robots, fractional calculus, formation control, sliding mode, consensus protocol

In this paper, an adaptive distributed formation controller for wheeled nonholonomic mobile robots is developed. The dynamical model of the robots is first derived by employing the Euler-Lagrange equation while taking into consideration the presence of disturbances and uncertainties in practical applications. Then, by incorporating fractional calculus in conjunction with fast terminal sliding mode control and consensus protocol, a robust distributed formation controller is designed to assure a fast and finite-time convergence of the robots towards the required formation pattern. Additionally, an adaptive mechanism is integrated to effectively counteract the effects of disturbances and uncertain dynamics. Moreover, the suggested control scheme's stability is theoretically proven through the Lyapunov theorem. Finally, simulation outcomes are given in order to show the enhanced performance and efficiency of the suggested control technique.

1. Introduction

Formation control of wheeled nonholonomic mobile robots has advanced significantly in the past few decades, and currently is regarded as a crucial research subject in the domains of multi-agent systems and robotics. This resulted from its potential in a variety of real-world applications, for example search and rescue

✉ Allaeddine Yahia DAMANI, email: damaniallaeddine@univ-blida.dz

[1]Laboratory of signal and image processing, Saad Dahlab University Blida 1, Blida, Algeria. ORCIDs: (A.Y.D) 0000-0002-3068-8518; (Z.A.B.) 0000-0003-3839-7544

[2]Center of Smart Robotics Research CEN, King Saud University, Riyadh, Saudi Arabia. ORCID (R.H.) 0000-0002-4648-1554

operations, exploration and object transportation. As well as the theoretical issues that arise during its control and modeling, such as the system nonlinearities, uncertainties and motion constraints must be considered. Numerous control approaches have been used to address the coordination of wheeled mobile robots in a formation. To name a few, behavior-based [1–3], potential-field [4, 5], consensus-based [6, 7], leader-follower [8–10] and virtual-structure [11–13] strategies.

Recently, consensus theory has been widely employed to design distributed formation control algorithms for multi-robot systems. Where the primary objective of using consensus protocol is to synchronize the motion of robots to reach a common position or velocity in order to establish a certain geometric shape. Different control strategies have been used alongside with consensus protocol to address the formation control problem, these include Model predictive control [14], Backstepping techniques [15, 16], Sliding mode control [17–19] and other control schemes [20, 21].

Sliding mode control outperforms the previously mentioned control schemes when it comes to dealing with system parameters variation, uncertainties and external disturbances. This superior performance has led to its widespread adoption in the control of multi-robot systems. The authors in [22] combine sliding mode control with fuzzy logic techniques to design an adaptive decentralized formation controller for a team of mobile robots under directed topologies with uncertain dynamics. In [23], consensus-based approach has been utilized in conjunction with sliding mode control to design a distributed controller for the formation of a team of unicycles. Authors in [24] investigate the formation control of multi nonholonomic wheeled robots. They develop a finite-time observer utilizing integral sliding mode method to estimate the robots velocities, then a dynamic output feedback controller has been used to drive all robots towards the predefined formation geometric configuration.

In the domain of control systems, fractional calculus theory has been utilized recently to control some dynamic systems [25, 26]. By incorporating the principles of fractional calculus (fractional order FO integral and derivatives), in combination with traditional control schemes such as PID [27] and sliding mode control SMC [28], the controller design process becomes more flexible and adjustable. Such combination can introduce an additional layer of adaptability to the control system, resulting in enhanced performance and increased efficiency in control operations.

Motivated by the above discussion, an adaptive distributed fractional fast terminal sliding mode controller ADFOFTSMC for multi-robots formation is suggested in this study. This control scheme can provide the following characteristics: graph theory and consensus-based techniques are used in this paper for representing the communication topology among the robots. Therefore, the control scheme design does not necessitate prior knowledge of the required bearing angle and separation distance for each robot in relation to its leader. Instead, the follower robot can get information only from its neighboring robots. The implementation of the fast terminal sliding mode control FTSMC method allows the robots to achieve

both rapid and finite-time convergence towards the desired pattern despite the existence of uncertain dynamics and disturbances. The inclusion of the FO derivatives into the FTSMC controller offers more freedom for control parameter selection, fine-tuning of the fractional orders leads to a desirable control performances. Additionally, an adaptive learning rule is used to estimate the bounded uncertainties and disturbances in the system. The performances of the suggested control method is evaluated through simulation results. The comparison findings indicate that the ADFOFTSMC is superior in terms of robustness, rapidity and accuracy.

The next sections of this paper are arranged as follows: In section 2 some concepts related to fractional calculus, graph theory, as well as the nonholonomic mobile robots dynamics and kinematics are explained. Then, the distributed formation controller synthesis is addressed in section 3. While section 4 presents the simulation results and discussions. Lastly, a conclusion is provided to summarize this study in section 5.

2. Preliminaries

2.1. Concepts on fractional calculus

Fractional calculus theory can be viewed as an extension of classical calculus. It generalizes the traditional concepts of integrals and derivatives to include non-integer or fractional orders; in fractional calculus, the derivative operator is denoted by $D^{\alpha} = \mathrm{d}^{\alpha}/\mathrm{d}t$ where α is a real number.

Definition 1. Using Riemann-Liouville (RL) definition, the α-order fractional derivative of function $f(t)$ over time can be expressed as follows [29]:

$$\begin{aligned} D^{\alpha} f(t) &= \frac{\mathrm{d}^{\alpha} f(t)}{\mathrm{d}t^{\alpha}} \\ &= \frac{1}{\Gamma(n-\alpha)} \left(\frac{\mathrm{d}^{n}}{\mathrm{d}t^{n}}\right) \int_{0}^{t} \frac{f(\tau)}{(t-\tau)^{\alpha+1-n}} \mathrm{d}\tau \,, \end{aligned} \tag{1}$$

where $(n-1 < \alpha < n)$ and $\Gamma(.)$ represent the Gamma function defined as:

$$\Gamma(\alpha) = \int_{0}^{\infty} e^{-t} t^{\alpha-1} \mathrm{d}t \,. \tag{2}$$

Propriety 1. *The n-th order derivative* $(\mathrm{d}^{n}/\mathrm{d}t^{n})$ *of* $f(t)$ *can be written by using the fractional derivative operator* D^{α} *as follows:*

$$D^{\alpha+n} f(t) = \frac{\mathrm{d}^{n}}{\mathrm{d}t^{n}} \left(D^{\alpha} f(t)\right) = D^{\alpha} \left(\frac{\mathrm{d}^{n} f(t)}{\mathrm{d}t^{n}}\right). \tag{3}$$

2.2. Algebraic graph theory

A useful tool for modeling multi-robot systems is the algebraic graph theory. It can be employed to represent the interaction between the robots, where the nodes of the graph are used to represent the robots and the edges represent the communication links.

Consider a multi-robot system consisting of n robot, and let $\mathcal{G} = (\mathcal{V}, \mathcal{E})$ be a graph with a directed topology where $\mathcal{V} = \{\nu_1, \nu_2, \ldots, \nu_n\}$ is the set of vertices (robots), and $\mathcal{E} \subseteq \mathcal{V} \times \mathcal{V}$ is the set of the links. The notation, $(\nu_i, \nu_j) \in \mathcal{E}$ means that the i-th robot can get information from the j-th robot, but not vice versa. For a digraph $\mathcal{G}$ the adjacency matrix is given as follows:

$$\mathcal{A} = \begin{bmatrix} a_{11} & a_{12} & \ldots & a_{1n} \\ a_{21} & a_{22} & \ldots & a_{2n} \\ \vdots & \vdots & \ddots & \vdots \\ a_{n1} & a_{n2} & \ldots & a_{nn} \end{bmatrix},$$

where the elements of $\mathcal{A}$ are given as follows:

$$\begin{aligned} a_{ij} &= 1, \quad (\nu_j, \nu_i) \in \mathcal{E}, \\ a_{ij} &= 0, \quad (\nu_j, \nu_i) \notin \mathcal{E}, \\ a_{ii} &= 0. \end{aligned}$$

Then, the digraph $\mathcal{G}$ Laplacian matrix is defined as follows:

$$\mathcal{L} = \mathcal{D} - \mathcal{A},$$

where $\mathcal{L} \in \mathcal{R}^{n \times n}$ and $\mathcal{D}$ is the in-degree diagonal matrix of $\mathcal{G}$ given by:

$$\mathcal{D} = \operatorname{diag}\left(\sum_{j=1}^{n} a_{ij} \right).$$

In this paper, a multi mobile robot system consists of n robots with only one leader that is addressed; the followers are denoted by indices $(1, 2, ..., n-1)$, while the leader robot is labeled with index n, and the exchange of information between the followers and the leader robot is considered to be unidirectional. In other words, the followers cannot send information to the leader robot.

Let $\bar{\mathcal{G}} = (\bar{\mathcal{V}}, \bar{\mathcal{E}})$ be a sub-graph of digraph G, then the adjacency matrix of $\bar{\mathcal{G}}$ can be written as:

$$\bar{\mathcal{A}} = \begin{bmatrix} \bar{a}_{11} & \bar{a}_{12} & \ldots & \bar{a}_{1(n-1)} \\ \bar{a}_{21} & \bar{a}_{22} & \ldots & \bar{a}_{2(n-1)} \\ \vdots & \vdots & \ddots & \vdots \\ \bar{a}_{(n-1)1} & \bar{a}_{(n-1)2} & \ldots & \bar{a}_{(n-1)(n-1)} \end{bmatrix}.$$

The sub-graph $\bar{\mathcal{G}}$ Laplacian matrix is written as follows:

$$\bar{\mathcal{L}} = \bar{\mathcal{D}} - \bar{\mathcal{A}}\,,$$

with in-degree matrix $\bar{\mathcal{D}} = \text{diag}\left(\sum_{j=1}^{n-1} \bar{a}_{ij}\right)$. The connection between the leader and the followers is represented by a diagonal matrix $\bar{\mathcal{B}}$, where $\bar{\mathcal{B}} = \text{diag}\{\bar{b}_1, \bar{b}_2, \ldots, \bar{b}_{n-1}\}$ and $\bar{b}_i = \bar{a}_{in}$, $i = 1, 2, \ldots, n-1$.

Lemma 1. *Let $\mathcal{G} = (\mathcal{V}, \mathcal{E})$ be a digraph, then the corresponding right eigenvector of the Laplacian matrix $\mathcal{L}$ associated with the eigenvalue* 0 *is the vector $\mathbf{1}_n$, only if the digraph $\mathcal{G}$ has a spanning tree, this mean that $\mathcal{L}\mathbf{1}_n = 0$.*

Lemma 2. *$\bar{\mathcal{L}}\mathbf{1}_{n-1} = 0$, if the sub-graph $\bar{\mathcal{G}}$ has a spanning tree [30], $(\bar{\mathcal{L}} + \bar{\mathcal{B}})$ is non-singular matrix and* $\text{Rank}(\bar{\mathcal{L}} + \bar{\mathcal{B}}) = n - 1$.

2.3. Modeling of nonholonomic mobile robot

Consider the nonholonomic wheeled robot illustrated in Fig. 1; the generalized coordinates of the robot are denoted by $q_i = [x_i \;\; y_i \;\; \theta_i]^T$ where θ_i is the heading angle, y_i and x_i are the robot head Cartesian coordinates. This type of robots is subjected to nonholonmic constraints given by equation:

$$\dot{y}_i \cos\theta_i - \dot{x}_i \sin\theta_i - d\dot{\theta}_i = 0\,. \tag{4}$$

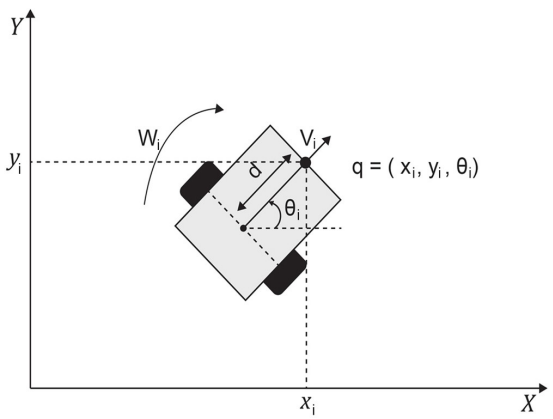

Fig. 1. Nonholonomic mobile robot

The distance between the head of the robot and its center of mass is denoted by d, using equation (4), the robot kinematic equation can be expressed as follows:

$$\dot{q}_i = \begin{bmatrix} \dot{x}_i \\ \dot{y}_i \\ \dot{\theta}_i \end{bmatrix} = \begin{bmatrix} \cos\theta_i & -d\sin\theta_i \\ \sin\theta_i & d\cos\theta_i \\ 0 & 1 \end{bmatrix} \begin{bmatrix} \nu_i \\ \omega_i \end{bmatrix} = \mathcal{J}(q_i)\mathcal{U}_i\,, \tag{5}$$

where ν_i denotes the robot linear velocity and ω_i is the angular velocity.

In this paper, the Euler-Lagrange equation is utilized to formulate the dynamic model of the i-th robot in the multi-robot system as follows:

$$M(q_i)\ddot{q}_i + V_m(q_i, \dot{q}_i)\dot{q}_i + \Delta_i = B(q_i)\tau_i \,. \tag{6}$$

The matrices and vectors described in equation (6) are given as follows:

$$B(q_i) = \frac{1}{r}\begin{bmatrix} \cos\theta_i & \cos\theta_i \\ \sin\theta_i & \sin\theta_i \\ R & -R \end{bmatrix},$$

$$\tau_i = \begin{bmatrix} \tau_{l_i} \\ \tau_{r_i} \end{bmatrix}, \quad \Delta_i = \begin{bmatrix} \Delta_{x_i} & \Delta_{y_i} & \Delta_{\theta_i} \end{bmatrix}^T,$$

$$V_m(q_i, \dot{q}_i) = \begin{bmatrix} 0 & 0 & md\dot{\theta}_i \cos\theta_i \\ 0 & 0 & md\dot{\theta}_i \sin\theta_i \\ 0 & 0 & 0 \end{bmatrix},$$

$$M(q_i) = \begin{bmatrix} m & 0 & md\sin\theta_i \\ 0 & m & -md\cos\theta_i \\ md\sin\theta_i & -md\cos\theta_i & I \end{bmatrix},$$

where Δ_i is a vector that consists of disturbances and uncertain dynamics, τ_i is the vector of control inputs, I denotes the total moment of inertia, r represent the wheel radius, m denotes the robot mass and $2R$ is the robot width.

By substituting the kinematic equation (5) into equation (6), the following robot dynamics are obtained:

$$\bar{M}(q_i)\dot{\mathcal{U}}_i + \bar{V}_m(q_i, \dot{q}_i)\mathcal{U}_i + \mathcal{J}^T(q_i)\Delta_i = \bar{B}(q_i)\tau_i \,, \tag{7}$$

with:

$$\bar{V}m(q_i, \dot{q}_i) = 0, \;\; \bar{B}(q_i) = \mathcal{J}^T(q_i)B(q_i)$$
$$\bar{M}(q_i) = \mathcal{J}^T(q_i)M(q_i)\mathcal{J}(q_i) \,,$$

under the assumption that $M(q_i)$ is invertible subject to $I - md^2 \neq 0$. Then equation (7) can be reformulated as follows:

$$\dot{\mathcal{U}}_i = \bar{M}^{-1}(q_i)\bar{B}(q_i)\tau_i - \bar{M}^{-1}(q_i)\mathcal{J}^T(q_i)\Delta_i \,. \tag{8}$$

The kinematic equation (5) can be re-written as:

$$\begin{bmatrix} \dot{x}_i \\ \dot{y}_i \end{bmatrix} = \begin{bmatrix} \cos\theta_i & -d\sin\theta_i \\ \sin\theta_i & d\cos\theta_i \end{bmatrix}\begin{bmatrix} \nu_i \\ \omega_i \end{bmatrix} = \mathcal{H}(\theta_i)\begin{bmatrix} \nu_i \\ \omega_i \end{bmatrix}. \tag{9}$$

Taking time derivative of (9), yields the following:

$$\begin{bmatrix} \ddot{x}_{hi} \\ \ddot{y}_{hi} \end{bmatrix} = \mathcal{H}_i(\theta_i) \left[\bar{M}^{-1}(q_i)\bar{B}(q_i)\tau_i - \bar{M}^{-1}(q_i)\mathcal{J}^T(q_i)\Delta_i \right] + \begin{bmatrix} \sigma_{1_i} \\ \sigma_{2_i} \end{bmatrix}, \tag{10}$$

where:

$$\begin{bmatrix} \sigma_{1_i} \\ \sigma_{2_i} \end{bmatrix} = \begin{bmatrix} -v_i\omega_i \sin(\theta_i) - d\omega_i^2 \cos(\theta_i) \\ v_i\omega_i \cos(\theta_i) - d\omega_i^2 \sin(\theta_i) \end{bmatrix} \tag{11}$$

by defining τ_i as follows:

$$\begin{bmatrix} \tau_{l_i} \\ \tau_{r_i} \end{bmatrix} = (\mathcal{H}_i(\theta_i)\bar{M}^{-1}(q_i)\bar{B}(q_i))^{-1} \begin{bmatrix} u_{x_i} - \sigma_{1_i} \\ u_{y_i} - \sigma_{2_i} \end{bmatrix}. \tag{12}$$

Then, the i-th robot simplified equivalent model can be given by substituting equation (12) in (10):

$$\begin{aligned} \begin{bmatrix} \dot{x}_i \\ \dot{y}_i \end{bmatrix} &= \begin{bmatrix} v_{x_i} \\ v_{y_i} \end{bmatrix}, \\ \begin{bmatrix} \dot{v}_{x_i} \\ \dot{v}_{y_i} \end{bmatrix} &= \begin{bmatrix} u_{x_i} \\ u_{y_i} \end{bmatrix} + \begin{bmatrix} \delta_{x_i} \\ \delta_{y_i} \end{bmatrix}, \end{aligned} \tag{13}$$

where (v_{yi}, v_{xi}) are the y-axis and x-axis robot velocities, respectively. (u_{xi}, u_{yi}) are the system control inputs and $(\delta_{xi}, \delta_{yi})$ denotes the bounded uncertainties described by:

$$\begin{bmatrix} \delta_{xi} \\ \delta_{yi} \end{bmatrix} = -\mathcal{H}_i(\theta_i)\bar{M}^{-1}(q_i)\mathcal{J}^T(q_i)\Delta_i \,. \tag{14}$$

Assumption 1. *The parametric uncertainties described in (14) are assumed to be bounded, which mean there exist a positive constants such that* $|\delta_{xi}| < \Delta_x$ *and* $|\delta_{yi}| < \Delta_y$.

3. Formation controller synthesis

In this section, the adaptive distributed formation control schemes are developed. The main objective is to force the robots to maintain a predefined pattern while achieving velocity consensus by exchanging information with local neighboring robots.

3.1. Formation error dynamics

Let $z_i = [x_i \; y_i]^T$, $v_i = [v_{x_i} \; v_{y_i}]^T$, $u_i = [u_{x_i} \; u_{y_i}]^T$ and $\delta_i = [\delta_{x_i} \; \delta_{y_i}]^T$. Then, the follower robots augmented state vector can be described as:

$$\begin{aligned} \dot{z} &= v \,, \\ \dot{v} &= u + \delta \,, \end{aligned} \tag{15}$$

with $z = \left[z_1^T\ z_2^T\ \dots\ z_{n-1}^T\right]^T$, $v = \left[v_1^T\ v_2^T\ \dots\ v_{n-1}^T\right]^T$, $u = \left[u_1^T\ u_2^T\ \dots\ u_{(n-1)}^T\right]^T$ and $\delta = \left[\delta_1^T\ \delta_2^T\ \dots\ \delta_{n-1}^T\right]^T$.
By defining the formation desired pattern positions as $f_i = [f_{ij}^x\ f_{ij}^y]^T$, then, the tracking error vector of the formation is defined as:

$$e = ((\bar{\mathcal{L}} + \bar{\mathcal{B}}) \otimes I_2)(z - f) - (\bar{\mathcal{B}} 1_{n-1} \otimes I_2) z_n \,, \tag{16}$$

where $I_2 \in R^{2\times 2}$ is the identity matrix, $\otimes$ is the Knocker product, $f = \left[f_1^T\ f_2^T\ \dots\ f_{n-1}^T\right]^T$, $e_i = [e_{x_i}\ e_{y_i}]^T$ and $e = \left[e_1^T\ e_2^T\ \dots\ e_{n-1}^T\right]^T$.

For each robot in the formation, the local tracking error for both x-axis and y-axis subsystems are presented as follows:

$$e_{x_i} = \sum_{j=1}^{n-1} \bar{a}_{ij}(x_i - x_j - f_{ij}^x) + \bar{b}_i(x_i - x_n) \,,$$

$$e_{y_i} = \sum_{j=1}^{n-1} \bar{a}_{ij}(y_i - y_j - f_{ij}^y) + \bar{b}_i(y_i - y_n) \,.$$

Taking the derivative of (16) yields the following tracking error dynamics:

$$\dot{e} = ((\bar{\mathcal{L}} + \bar{\mathcal{B}}) \otimes I_2) v - (\bar{\mathcal{B}} 1_{n-1} \otimes I_2) v_n \,. \tag{17}$$

Hence, the second derivative of equation (16) becomes:

$$\begin{aligned} \ddot{e} = &\left(\left(\bar{\mathcal{L}} + \bar{\mathcal{B}}\right) \otimes I_2\right) u + \left(\left(\bar{\mathcal{L}} + \bar{\mathcal{B}}\right) \otimes I_2\right) \delta \\ &- \left(\bar{\mathcal{B}} 1_{n-1} \otimes I_2\right) u_n \,. \end{aligned} \tag{18}$$

3.2. FO fast terminal sliding mode controller design

Sliding mode control composed of two control actions, the switching control $u_{sw}(t)$ and the equivalent control $u_{eq}(t)$. Consequently, the total control scheme can be expressed as follows:

$$u(t) = u_{eq}(t) + u_{sw}(t) \,, \tag{19}$$

with $u_{eq} = \left[u_{1,eq}^T\ u_{2,eq}^T\ \dots\ u_{(n-1),eq}^T\right]^T$ and $u_{sw} = \left[u_{1,sw}^T\ u_{2,sw}^T\ \dots\ u_{(n-1),sw}^T\right]^T$ where $u_{i,eq} = [u_{xi,eq}\ u_{yi,eq}]^T$ and $u_{i,sw} = [u_{xi,sw}\ u_{yi,sw}]^T$
First, the sliding manifold is defined as follows:

$$S = \dot{e} + \alpha_1 e + \alpha_2 e^{\beta_1/\beta_2} \,, \tag{20}$$

where $\alpha_1 > 0, \alpha_2 > 0$, β_1, β_2 are positive odd integers, with $\beta_1 < \beta_2 < 2\beta_1$, and $S = \left[S_1^T\ S_2^T\ \dots\ S_{(n-1)}^T\right]^T$ is the vector of sliding surfaces with $S_i = [S_{x_i}\ S_{y_i}]^T$.

Lemma 3. *The time interval required for any initial state $e \neq 0$ to reach the equilibrium state $e = 0$ along the sliding surface defined in (20), can be calculated as:*

$$t_f = \frac{\beta_2}{\alpha_1(\beta_2 - \beta_1)} \ln \frac{\alpha_1 (e_0)^{\left(1-\frac{\beta_1}{\beta_2}\right)} + \alpha_2}{\alpha_2} . \tag{21}$$

By using FO definition and Propriety 1, equation (20) can be re-written as:

$$S = D^{\alpha} e + \alpha_1 e + \alpha_2 e^{\beta_1/\beta_2} . \tag{22}$$

The sliding surface S first derivative can be given as:

$$\begin{aligned} \dot{S} &= D^{\alpha+1} e + \alpha_1 \dot{e} + \alpha_2(\beta_1/\beta_2)\dot{e}e^{(\beta_1/\beta_2)-1} , \\ \dot{S} &= ((\bar{\mathcal{L}} + \bar{\mathcal{B}}) \otimes I_2)u + ((\bar{\mathcal{L}} + \bar{\mathcal{B}}) \otimes I_2)\delta - (\bar{\mathcal{B}} 1_{n-1} \otimes I_2)u_n \\ &\quad + \alpha_1 \dot{e} + \alpha_2(\beta_1/\beta_2)\dot{e}e^{(\beta_1/\beta_2)-1} . \end{aligned} \tag{23}$$

In the absence of system uncertainties, the derivative of S becomes:

$$\begin{aligned} \dot{S} = ((\bar{\mathcal{L}} + \bar{\mathcal{B}}) \otimes I_2)u - (\bar{\mathcal{B}} 1_{n-1} \otimes I_2)u_n \\ + \alpha_1 \dot{e} + \alpha_2(\beta_1/\beta_2)\dot{e}e^{(\beta_1/\beta_2)-1} . \end{aligned} \tag{24}$$

Hence, the equivalent control law can be derived by solving $\dot{S} = 0$:

$$u_{eq} = -((\bar{\mathcal{L}} + \bar{\mathcal{B}})^{-1} \left[-(\bar{\mathcal{B}} 1_{n-1} \otimes I_2)u_n + \alpha_1 \dot{e} + \alpha_2(\beta_1/\beta_2)\dot{e}e^{(\beta_1/\beta_2)-1} \right] , \tag{25}$$

and the switching control action is defined as follows:

$$u_{sw} = -(\bar{\mathcal{L}} + \bar{\mathcal{B}})^{-1} \left[\mathcal{K} \operatorname{sign}(S) \right] , \tag{26}$$

where sign(.) is the Signum function and $\mathcal{K}$ is a positive gain.

3.3. Design of adaptive fractional order fast terminal sliding mode controller

In practical scenarios, the measurement of accurate values of uncertainties and disturbances can be challenging. Therefore, an adaptive mechanism is designed to estimate the upper bounds of this factors.

First, let $\hat{\Delta} = \left[\hat{\Delta}_1^T \ \hat{\Delta}_2^T \ \dots \ \hat{\Delta}_{(n-1)}^T \right]^T$ be the vector of estimated uncertainties bounds with $\hat{\Delta}_i = [\hat{\Delta}_{x_i} \ \hat{\Delta}_{y_i}]^T$. Then, the error of estimation is given as:

$$\tilde{\Delta} = \Delta - \hat{\Delta} , \tag{27}$$

where $\tilde{\Delta} = \left[\tilde{\Delta}_1^T \ \tilde{\Delta}_2^T \ \dots \ \tilde{\Delta}_{(n-1)}^T \right]^T$, $\Delta = \left[\Delta_1^T \ \Delta_2^T \ \dots \ \Delta_{(n-1)}^T \right]^T$ with $\tilde{\Delta}_i = [\tilde{\Delta}_{x_i} \ \tilde{\Delta}_{y_i}]^T$ and $\Delta_i = [\Delta_{x_i} \ \Delta_{y_i}]^T$. Consider the following adaptive rule:

$$\dot{\hat{\Delta}} = 2\gamma((\bar{\mathcal{L}} + \bar{\mathcal{B}}) \otimes I_2)|S| , \tag{28}$$

where $\gamma = [\gamma_1\ \gamma_2 \ldots \gamma_{n-1}]$ and $\gamma_i > 0$.
Therefore, the final formation controller can be expressed as follows:

$$u = u_{eq} - \hat{\Delta}\,\mathrm{sign}(S)\,. \tag{29}$$

Theorem 1. *Assuming that the digraph $\mathcal{G}$ associated with the multi-robots system described in (15) have a spanning tree. The formation objective can be accomplished and the tracking errors described in (16) will asymptotically reach the origin in finite-time, by utilizing the proposed controller (29) with the adaptive algorithm (28).*

Proof. Let V be a candidate Lyapunov function:

$$V = \frac{1}{2}S^T S + \frac{1}{2\gamma}\tilde{\Delta}^T\tilde{\Delta}\,. \tag{30}$$

Then, V first derivative is written as follows:

$$\begin{aligned}\dot{V} &= \frac{1}{2}S^T\dot{S} + \frac{1}{2\gamma}\tilde{\Delta}^T\dot{\tilde{\Delta}}\,,\\ &= \frac{1}{2}S^T\dot{S} - \frac{1}{2\gamma}\tilde{\Delta}^T\dot{\hat{\Delta}}\,.\end{aligned} \tag{31}$$

Substituting equation (23) into (31) leads to:

$$\begin{aligned}\dot{V} = S^T\Big[&((\bar{\mathcal{L}}+\bar{\mathcal{B}})\otimes I_2)u + ((\bar{\mathcal{L}}+\bar{\mathcal{B}})\otimes I_2)\delta - (\bar{\mathcal{B}}1_{n-1}\otimes I_2)u_n\\ &+\ \alpha_1\dot{e} + \alpha_2(\beta_1/\beta_2)\dot{e}e^{(\beta_1/\beta_2)-1}\Big] - \frac{1}{2\gamma}\tilde{\Delta}^T\dot{\hat{\Delta}}\,.\end{aligned} \tag{32}$$

Substituting the control law (29) into equality (32) yields the following:

$$\dot{V} = S^T\left[((\bar{\mathcal{L}}+\bar{\mathcal{B}})\otimes I_2)\delta - ((\bar{\mathcal{L}}+\bar{\mathcal{B}})\otimes I_2)\hat{\Delta}\,\mathrm{sign}(S)\right] - \frac{1}{2\gamma}\tilde{\Delta}^T\dot{\hat{\Delta}}\,. \tag{33}$$

Using Assumption 1 and the adaptive rule in equation (28), gives the following:

$$\begin{aligned}\dot{V} &= S^T\left[((\bar{\mathcal{L}}+\bar{\mathcal{B}})\otimes I_2)(\delta - \hat{\Delta}\,\mathrm{sign}(S))\right] - \tilde{\Delta}^T((\bar{\mathcal{L}}+\bar{\mathcal{B}})\otimes I_2)|S|\\ &\leqslant ((\bar{\mathcal{L}}+\bar{\mathcal{B}})\otimes I_2)(|S|\otimes I_2)(\Delta - \hat{\Delta} - \tilde{\Delta}) = 0\,.\end{aligned} \tag{34}$$

Based on equation (34), it can be concluded that the tracking errors of the formation will asymptotically reach 0 in a finite-time, and Theorem 1 proof is completed. □

According to Theorem 1 the formation of multi-robots system (15) can be established by using the control scheme (29). Therefore, equation (16) can be described as follows:

$$((\bar{\mathcal{L}}+\bar{\mathcal{B}})\otimes I_2)(z - f) = (\bar{\mathcal{B}}1_{n-1}\otimes I_2)z_n\,. \tag{35}$$

Assuming $\mathcal{G}$ has a directed spanning tree and by using Lemma 2, we obtain the following:

$$\begin{aligned}\left((\bar{\mathcal{L}}+\bar{\mathcal{B}})\otimes I_2\right)(z-f) &= (\bar{\mathcal{B}}1_{n-1}\otimes I_2)z_n\,,\\ \left((\bar{\mathcal{L}}+\bar{\mathcal{B}})\otimes I_2\right)(z-f) &= ((\bar{\mathcal{L}}+\bar{\mathcal{B}})\otimes I_2)(1_{n-1}\otimes I_2)z_n\,,\\ (z-f) &= (1_{n-1}\otimes I_2)z_n\,.\end{aligned} \tag{36}$$

From equation (36), one can conclude that positions consensus can be established when the tracking errors of the formation converges to zero.

4. Simulation results

Numerical simulation based on MATLAB environment is presented in this section. A multi-robot system consisted of six nonholonomic wheeled mobile robots is considered in this simulation example. The parameters of each robot are selected as: $d = 0.04$ m, $R = 0.0265$ m, $r = 0.02$ m, $m = 0.032$ kg and $I = 1.7^{-4}$ kg.m^2.

A communication graph G with a directed topology is employed for modeling the information exchange among robots. The representation of G is depicted in Fig. 2, where the node labeled with number 6 represents the leader robot and the reset of vertices (1–5) are the followers.

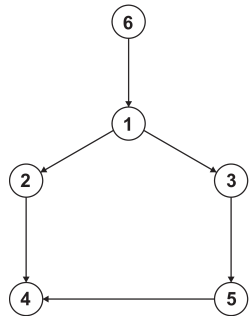

Fig. 2. Formation communication graph

The matrices $\mathcal{L}, \mathcal{A}$ and $\mathcal{B}$ associated with G are given as follows:

$$\mathcal{L} = \begin{bmatrix} 1 & 0 & 0 & 0 & 0 & -1 \\ -1 & 1 & 0 & 0 & 0 & 0 \\ -1 & 0 & 1 & 0 & 0 & 0 \\ 0 & -1 & 0 & 2 & -1 & 0 \\ 0 & 0 & -1 & 0 & 1 & 0 \\ 0 & 0 & 0 & 0 & 0 & 0 \end{bmatrix},$$

$$\mathcal{A} = \begin{bmatrix} 0 & 0 & 0 & 0 & 0 & 1 \\ 1 & 0 & 0 & 0 & 0 & 0 \\ 1 & 0 & 0 & 0 & 0 & 0 \\ 0 & 1 & 0 & 0 & 1 & 0 \\ 0 & 0 & 1 & 0 & 0 & 0 \\ 0 & 0 & 0 & 0 & 0 & 0 \end{bmatrix},$$

$$\mathcal{B} = \begin{bmatrix} 1 & 0 & 0 & 0 & 0 & 0 \\ 0 & 0 & 0 & 0 & 0 & 0 \\ 0 & 0 & 0 & 0 & 0 & 0 \\ 0 & 0 & 0 & 0 & 0 & 0 \\ 0 & 0 & 0 & 0 & 0 & 0 \\ 0 & 0 & 0 & 0 & 0 & 0 \end{bmatrix}.$$

To examine the efficacy of the suggested ADFOFTSMC method, a comparative study is carried out, where ADFOFTSMC is compared to the second order consensus algorithm SOCA proposed in [31], and the distributed sliding mode control DSMC in [32].

The suggested controller design parameters are chosen as follows: $\alpha_1 = \frac{1}{2}$, $\alpha_2 = 1$, $\beta_1 = 7$, $\beta_2 = 9$, $\alpha = 0.78$ and $\gamma = 10$. The uncertainties terms Δ_i in equation (6) are supposed be uniformly randomly distributed between -0.025 and 0.025.

In order to establish a Hexagon-like formation the robots desired postures are defined as: $f_{x_i} = [-0.125 \ -0.375 \ -0.5 \ -0.375 \ -0.125]$ and $f_{y_i} = [0.2165 \ 0.2165 \ 0 \ -0.2165 \ -0.2165]$. Fig. 3 shows the desired formation shape.

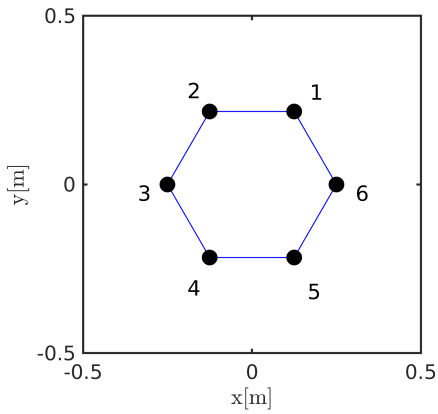

Fig. 3. Desired formation pattern

The leader robot is assumed to move in a sinusoidal motion with $v_{x_i} = 0.25$ m/s, $v_{y_i} = 0.05\cos(.25\pi t)$ m/s and the robots initial positions are selected as follows: $x_i = [0.10 \ -0.25 \ -0.50 \ -0.4 \ -0.1 \ 0.25]$ and $y_i = [0.4 \ 0.5 \ 0.45 \ -0.3 \ -0.5 \ 0]$. Furthermore, the formation tracking performances are analyzed using the following error indexes ISE $= \int_0^T E(t)^2 \mathrm{d}t$, ITSE $= \int_0^T tE(t)^2 \mathrm{d}t$, RMSE $= \sqrt{\frac{1}{T}\int_0^T E(t)^2 \mathrm{d}t}$, ITAE $= \int_0^T t|E(t)|\mathrm{d}t$, IAE $= \int_0^T |E(t)|\mathrm{d}t$, where T is the simulation time and $E(t)$ is defined in (37). Table 1 shows the tracking performance results.

$$E(t) = \sum_{i=1}^{5} |e_{x_i}(t)| + \sum_{i=1}^{5} |e_{y_i}(t)| \,. \tag{37}$$

Table 1. Formation tracking performances

$E(t)$	SOCA [31]	DSMC [32]	ADFOFTSMC
RMSE	384.50×10^{-3}	372.40×10^{-3}	280.30×10^{-3}
ISE	2.2175×10^{3}	2.0801×10^{3}	1.1783×10^{3}
ITSE	1.6769×10^{3}	1.6120×10^{3}	0.3996×10^{3}
ITAE	6.3164×10^{3}	5.8919×10^{3}	1.2690×10^{3}
IAE	2.7677×10^{3}	2.6831×10^{3}	1.2682×10^{3}

The simulation results for the second order consensus algorithm are illustrated in Figs. 4–6, where Fig. 4 presents the formation desired pattern at several moments, Fig. 5 depict the formation tracking errors (e_{x_i}, e_{y_i}) and the robots control inputs (τ_{l_i}, τ_{r_i}) are presented in Fig. 6, while the obtained results of the DSMC are presented in Figs. 7–9, respectively. Finally, the proposed ADFOFTSMC results are depicted in Figs. 10–12.

The simulation results presented in Fig. 4, Fig. 7 and Fig. 10 demonstrate the successful achievement of the formation using all control strategies. Nevertheless, it is evident that the utilization of the proposed ADFOFTMSC leads to a faster convergence rate of the robots towards the desired formation pattern. Meanwhile, the evaluation of the tracking errors of the robots, depicted in Fig. 5, Fig. 8 and Fig. 11, clearly demonstrates that the SOCA and DSMC methods exhibit inferior performance in terms of disturbances and uncertainties rejection when compared to the proposed control method. Additionally, the ADFOFTMSC control technique has the lowest minimal error tracking values when compared to SOCA and DSMC methods, as shown by the comparison between the tracking error indices shown in Table 1.

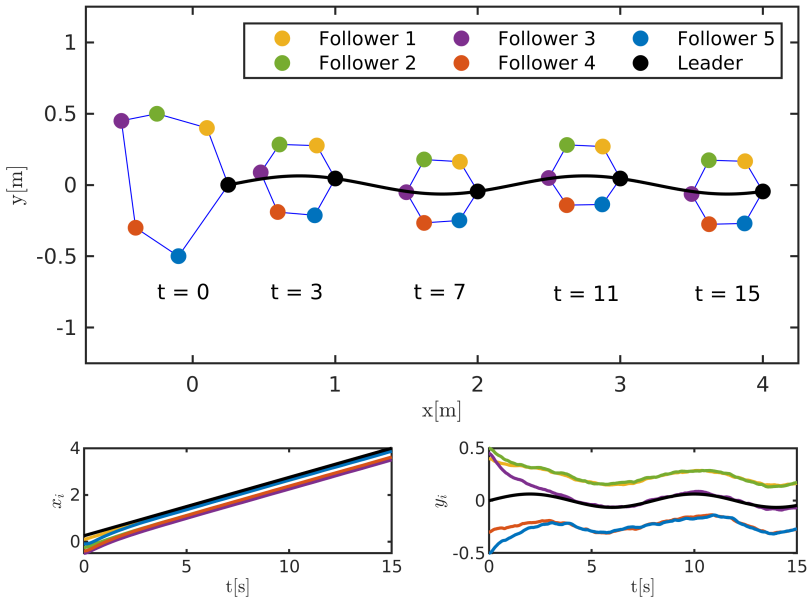

Fig. 4. Desired formation pattern at several moment with the leader trajectory (black line), based on SOCA [31]

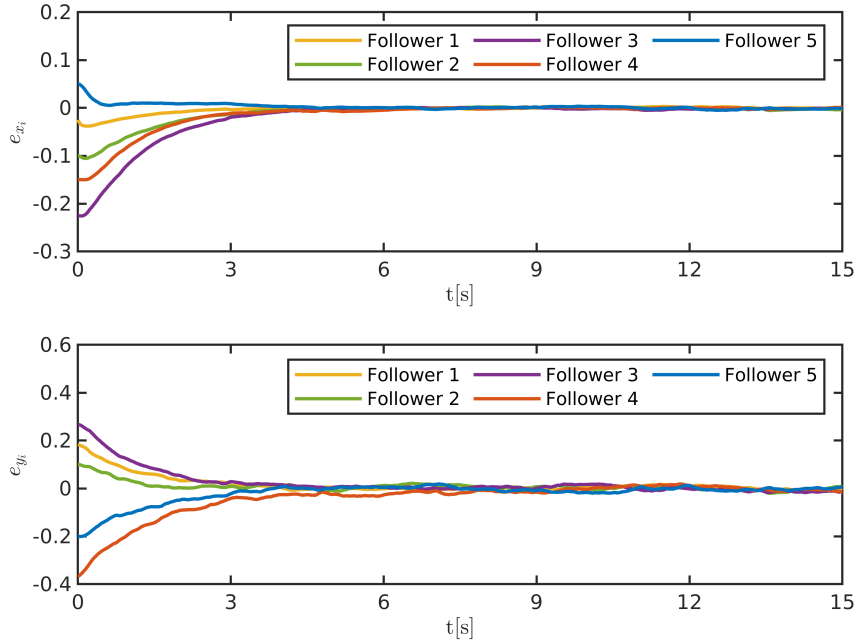

Fig. 5. Followers tracking errors, based on SOCA [31]

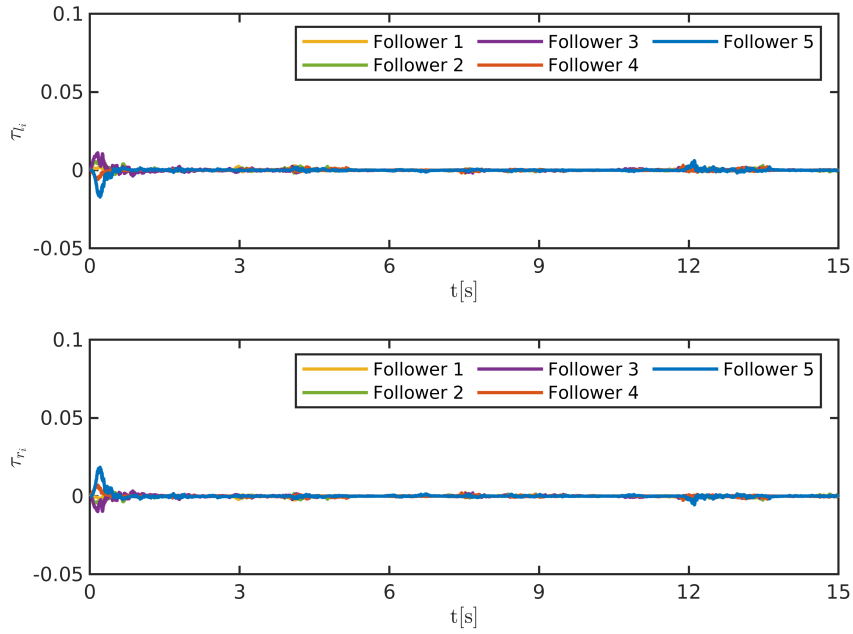

Fig. 6. Followers control inputs, based on SOCA [31]

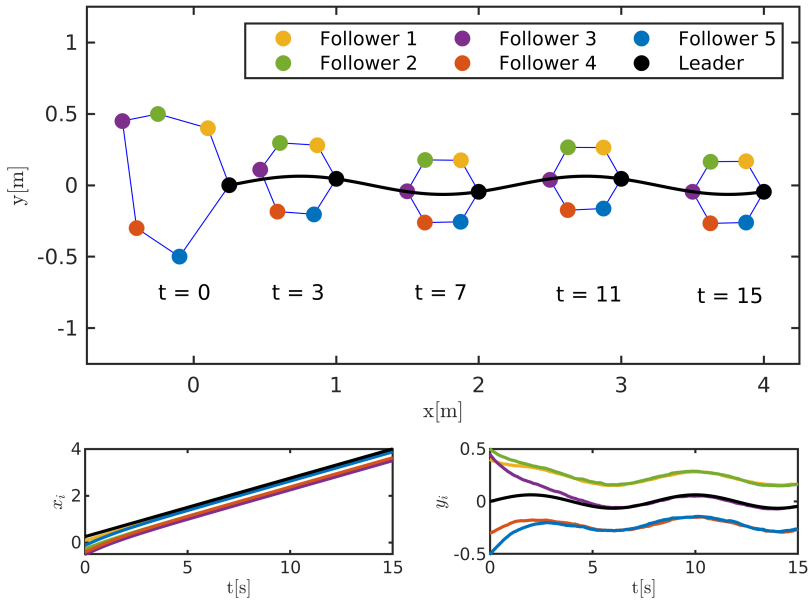

Fig. 7. Desired formation pattern at several moment with the leader trajectory (black line), based on DSMC [32]

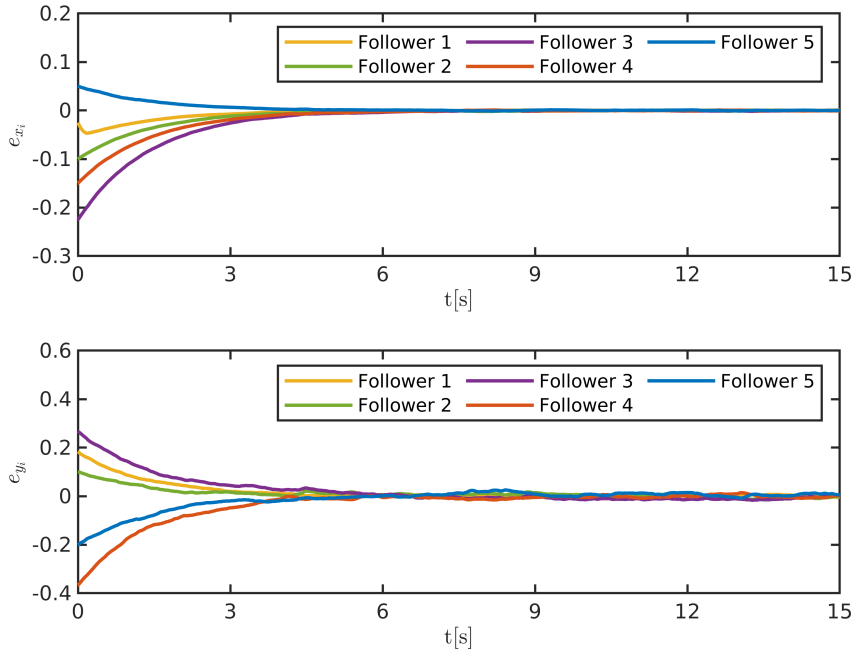

Fig. 8. Followers tracking errors, based on DSMC [32]

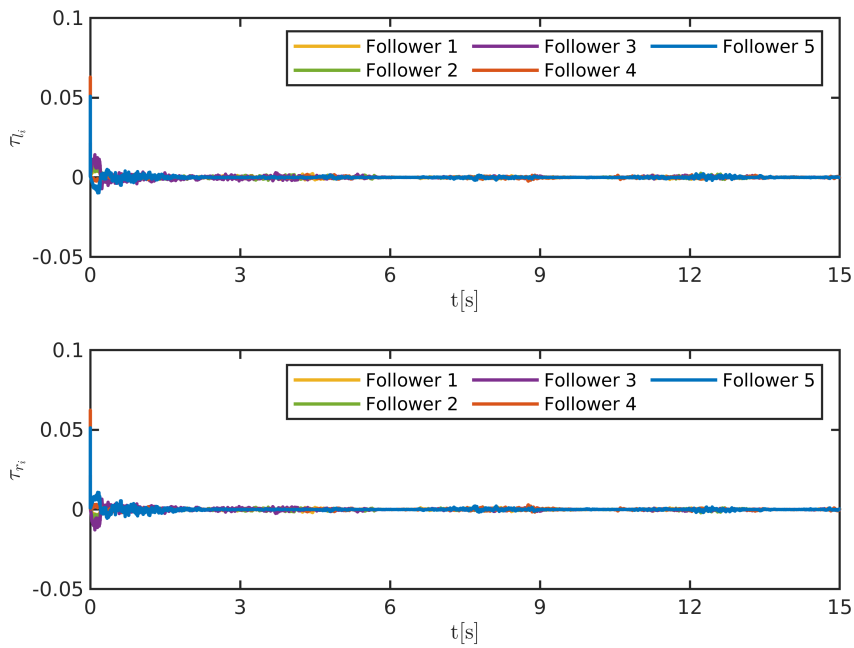

Fig. 9. Followers control inputs, based on DSMC [32]

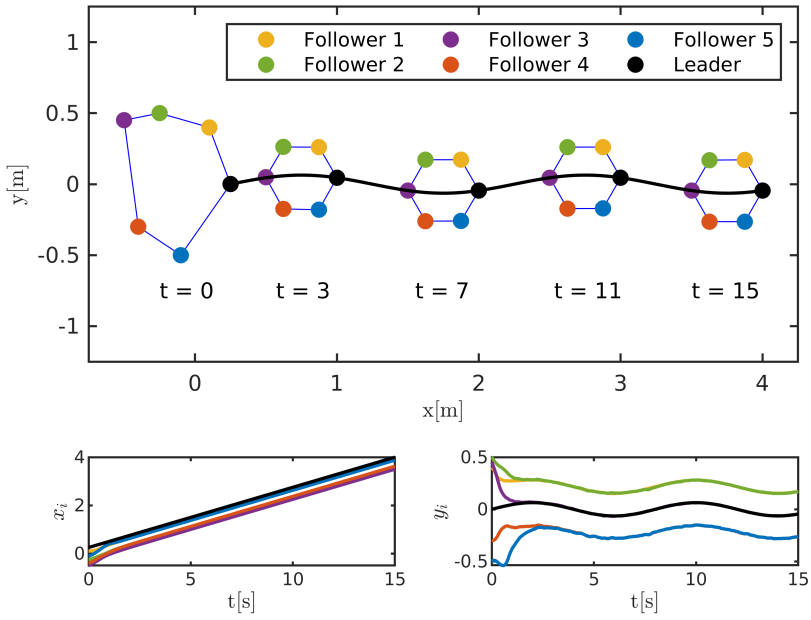

Fig. 10. Desired formation pattern at several moment with the leader trajectory (black line), based on ADFOFTMSC

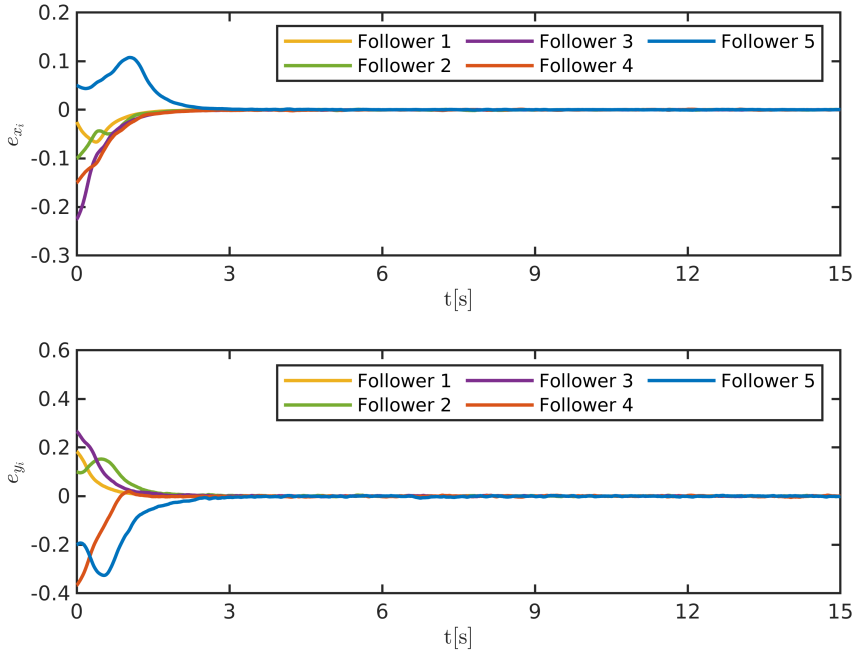

Fig. 11. Followers tracking errors, based on ADFOFTMSC

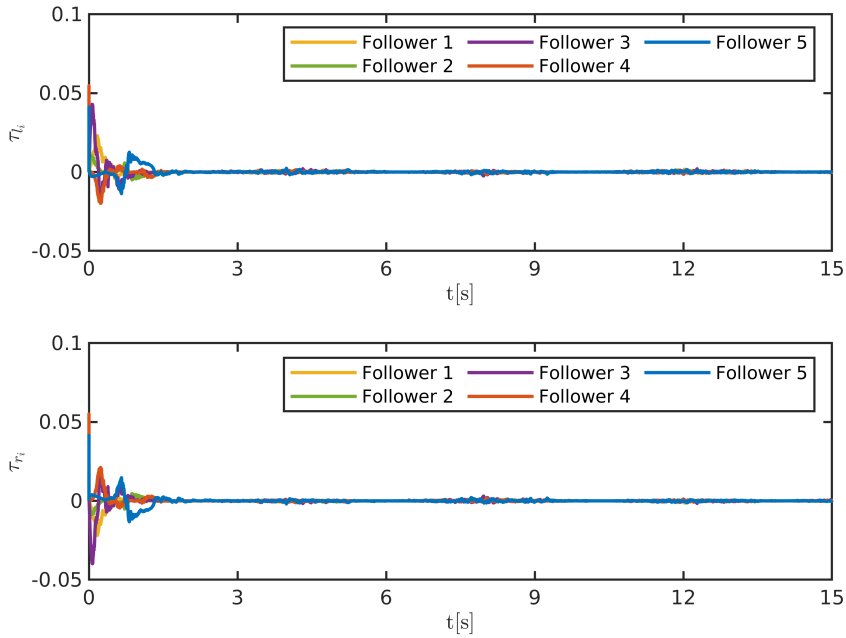

Fig. 12. Followers control inputs, based on ADFOFTMSC

The aforementioned comparison results illustrate that the ADFOFTMSC method surpasses the other used control techniques in terms of control performances. The proposed controller can ensure superior robustness against system uncertainties and disturbances and achieves a higher tracking accuracy with a faster convergence rate, which lead to an accurate and efficient formation control of robots.

5. Conclusion

An adaptive distributed formation controller for wheeled nonholonomic mobile robots is developed in this paper. The dynamic model of the robots is formulated using the Euler-Lagrange equation, with accounting the presence of bounded disturbances and unmodeled dynamics in practical scenarios. Through the integration of fractional calculus with fast terminal sliding mode control and consensus algorithm, a robust distributed formation controller has been designed to drive the followers robots to establish the predefined formation geometric shape while tracking their leader. Furthermore, an adaptive mechanism is devised to effectively mitigate the impact of uncertainties and disturbances. The suggested control scheme stability has been analyzed utilizing the Lyapunov theorem. The efficiency of the suggested control technique has been investigated through conducting a comparative study. The outcomes highlight the superior performance of the suggested controller in terms of formation accuracy, robustness and convergence.

References

[1] D. Xu, X. Zhang, Z. Zhu, C. Chen, and P. Yang. Behavior-based formation control of swarm robots. *Mathematical Problems in Engineering*, 2014:205759, 2014. doi: 10.1155/2014/205759.

[2] G. Lee and D. Chwa. Decentralized behavior-based formation control of multiple robots considering obstacle avoidance. *Intelligent Service Robotics*, 11:127–138, 2018. doi: 10.1007/s11370-017-0240-y.

[3] N. Hacene and B. Mendil. Behavior-based autonomous navigation and formation control of mobile robots in unknown cluttered dynamic environments with dynamic target tracking. *International Journal of Automation and Computing*, 18:766–786, 2021. doi: 10.1007/s11633-020-1264-x.

[4] Z. Pan, D. Li, K. Yang, and H. Deng. Multi-robot obstacle avoidance based on the improved artificial potential field and pid adaptive tracking control algorithm. *Robotica*, 37(11):1883–1903, 2019. doi: 10.1017/S026357471900033X.

[5] A.D. Dang, H.M. La, T. Nguyen, and J. Horn. Formation control for autonomous robots with collision and obstacle avoidance using a rotational and repulsive force–based approach. *International Journal of Advanced Robotic Systems*, 16(3):1729881419847897, 2019. doi: 10.1177/1729881419847897.

[6] M. Maghenem, A. Loría, E. Nuno, and E. Panteley. Consensus-based formation control of networked nonholonomic vehicles with delayed communications. *IEEE Transactions on Automatic Control*, 66(5):2242–2249, 2020. doi: 10.1109/TAC.2020.3005668.

[7] J.G. Romero, E. Nuño, E. Restrepo, and I. Sarras. Global consensus-based formation control of nonholonomic mobile robots with time-varying delays and without velocity measurements. *IEEE Transactions on Automatic Control*, 2023. doi: 10.1109/TAC.2023.3264744.

[8] S.-L. Dai, S. He, X. Chen, and X. Jin. Adaptive leader–follower formation control of nonholonomic mobile robots with prescribed transient and steady-state performance. *IEEE Transactions on Industrial Informatics*, 16(6):3662–3671, 2019. doi: 10.1109/TII.2019.2939263.

[9] J. Hirata-Acosta, J. Pliego-Jiménez, C. Cruz-Hernádez, and R. Martínez-Clark. Leader-follower formation control of wheeled mobile robots without attitude measurements. *Applied Sciences*, 11(12):5639, 2021. doi: 10.3390/app11125639.

[10] X. Liang, H. Wang, Y.-H. Liu, Z. Liu, and W. Chen. Leader-following formation control of nonholonomic mobile robots with velocity observers. *IEEE/ASME Transactions on Mechatronics*, 25(4):1747–1755, 2020. doi: 10.1109/TMECH.2020.2990991.

[11] X. Chen, F. Huang, Y. Zhang, Z. Chen, S. Liu, Y. Nie, J. Tang, and S. Zhu. A novel virtual-structure formation control design for mobile robots with obstacle avoidance. *Applied Sciences*, 10(17):5807, 2020. doi: 10.3390/app10175807.

[12] L. Dong, Y. Chen, and X. Qu. Formation control strategy for nonholonomic intelligent vehicles based on virtual structure and consensus approach. *Procedia Engineering*, 137:415–424, 2016. doi: 10.1016/j.proeng.2016.01.276.

[13] N. Nfaileh, K. Alipour, B. Tarvirdizadeh, and A. Hadi. Formation control of multiple wheeled mobile robots based on model predictive control. *Robotica*, 40(9):3178–3213, 2022. doi: 10.1017/S0263574722000121.

[14] H. Xiao, C.L.P. Chen, G. Lai, D. Yu, and Y. Zhang. Integrated nonholonomic multi-robot consensus tracking formation using neural-network-optimized distributed model predictive control strategy. *Neurocomputing*, 518:282–293, 2023. doi: 10.1016/j.neucom.2022.11.007.

[15] W. Wang, J. Huang, C. Wen, and H. Fan. Distributed adaptive control for consensus tracking with application to formation control of nonholonomic mobile robots. *Automatica*, 50(4):1254–1263, 2014. doi: 10.1016/j.automatica.2014.02.028.

[16] Y.H. Moorthy and S. Joo. Distributed leader-following formation control for multiple nonholonomic mobile robots via bioinspired neurodynamic approach. *Neurocomputing*, 492:308–321, 2022. doi: 10.1016/j.neucom.2022.04.001.

[17] S. Ik Han. Prescribed consensus and formation error constrained finite-time sliding mode control for multi-agent mobile robot systems. *IET Control Theory & Applications*, 12(2):282–290, 2018. doi: 10.1049/iet-cta.2017.0351.

[18] C.-C. Tsai, Y.-X. Li, and F.-C. Tai. Backstepping sliding-mode leader-follower consensus formation control of uncertain networked heterogeneous nonholonomic wheeled mobile multirobots. In *2017 56th Annual Conference of the Society of Instrument and Control Engineers of Japan (SICE)*, pages 1407–1412. IEEE, 2017. doi: 10.23919/SICE.2017.8105661.

[19] R. Rahmani, H. Toshani, and S. Mobayen. Consensus tracking of multi-agent systems using constrained neural-optimiser-based sliding mode control. *International Journal of Systems Science*, 51(14):2653–2674, 2020. doi: 10.1080/00207721.2020.1799257.

[20] R. Afdila, F. Fahmi, and A. Sani. Distributed formation control for groups of mobile robots using consensus algorithm. *Bulletin of Electrical Engineering and Informatics*, 12(4):2095–2104, 2023. doi: 10.11591/eei.v12i4.3869.

[21] L.-D. Nguyen, H.-L. Phan, H.-G. Nguyen, and T.-L. Nguyen. Event-triggered distributed robust optimal control of nonholonomic mobile agents with obstacle avoidance formation, input constraints and external disturbances. *Journal of the Franklin Institute*, 360(8):5564–5587, 2023. doi: 10.1016/j.jfranklin.2023.02.033.

[22] Y.-H. Chang, C.-Y. Yang, W.-S. Chan, H.-W. Lin, and C.-W. Chang. Adaptive fuzzy sliding-mode formation controller design for multi-robot dynamic systems. *International Journal of Fuzzy Systems*, 16(1):121–131, 2014.

[23] X. Chu, Z. Peng, G. Wen, and A. Rahmani. Robust fixed-time consensus tracking with application to formation control of unicycles. *IET Control Theory & Applications*, 12(1):53–59, 2018. doi: 10.1049/iet-cta.2017.0319.

[24] Y. Cheng, R. Jia, H. Du, G. Wen, and W. Zhu. Robust finite-time consensus formation control for multiple nonholonomic wheeled mobile robots via output feedback. *International Journal of Robust and Nonlinear Control*, 28(6):2082–2096, 2018. doi: 10.1002/rnc.4002.

[25] Y. Xie, X. Zhang, W. Meng, S. Zheng, L. Jiang, J. Meng, and S. Wang. Coupled fractional-order sliding mode control and obstacle avoidance of a four-wheeled steerable mobile robot. *ISA Transactions*, 108:282–294, 2021. doi: 10.1016/j.isatra.2020.08.025.

[26] J. Bai, G. Wen, A. Rahmani, and Y. Yu. Distributed formation control of fractional-order multi-agent systems with absolute damping and communication delay. *International Journal of Systems Science*, 46(13):2380–2392, 2015. doi: 10.1080/00207721.2014.998411.

[27] R. Cajo, M. Guinaldo, E. Fabregas, S. Dormido, D. Plaza, R. De Keyser, and C. Ionescu. Distributed formation control for multiagent systems using a fractional-order proportional–integral structure. *IEEE Transactions on Control Systems Technology*, 29(6):2738–2745, 2021. doi: 10.1109/TCST.2021.3053541.

[28] K.K. Ayten, M.H. Çiplak, and A. Dumlu. Implementation a fractional-order adaptive model-based pid-type sliding mode speed control for wheeled mobile robot. *Proceedings of the Institution of Mechanical Engineers, Part I: Journal of Systems and Control Engineering*, 233(8):1067–1084, 2019. doi: 10.1177/0959651819847395.

[29] D. Baleanu, K. Diethelm, E. Scalas, and J.J. Trujillo. *Fractional Calculus: Models and Numerical Methods*, volume 3. World Scientific, 2012.

[30] Y.-H. Chang, C.-W. Chang, C.-L. Chen, and C.-W. Tao. Fuzzy sliding-mode formation control for multirobot systems: design and implementation. *IEEE Transactions on Systems, Man, and Cybernetics, Part B (Cybernetics)*, 42(2):444–457, 2011. doi: 10.1109/TSMCB.2011.2167679.

[31] W. Ren and Beard R.W. Distributed consensus in multi-vehicle cooperative control: Theory and applications. *Springer, London*, 2007.

[32] T.-L. Liao, J.-J. Yan, and W.-S. Chan. Distributed sliding-mode formation controller design for multirobot dynamic systems. *Journal of Dynamic Systems, Measurement, and Control*, 139(6):061008, 2017. doi: 10.1115/1.4035614.